ANN-based Model Predictive Control for Hybrid Energy Storage Systems in DC Microgrid

Dongran Song, Asifa Yousaf, Javeria Noor, Yuan Cao, Mi Dong, Jian Yang, Rizk M. Rizk-Allah, M. H. Elkholy, and M. Talaat

***Abstract*—Hybrid energy storage system (HESS) is an effective solution to address power imbalance problems caused by variability of renewable energy resources and load fluctuations in DC microgrids. The goal of HESS is to efficiently utilize different types of energy storage systems, each with its unique characteristics. Normally, the energy management of HESS relies on centralized control methods, which have limitations in flexibility, scalability, and reliability. This paper proposes an innovative artificial neural network (ANN) based model predictive control (MPC) method, integrated with a decentralized power-sharing strategy for HESS. In the proposed technique, MPC is employed as an expert to provide data to train the ANN. Once the ANN is finely tuned, it is directly utilized to control the DC-DC converters, eliminating the need for the extensive computations typically required by conventional MPC. In the proposed control scheme, virtual resistance droop control for fuel cell (FC) and virtual capacitance droop control for battery are designed in a decentralized manner to achieve power-sharing, enhance lifespan, and ensure HESS stability. As a result, the FC is able to support steady state loads, while the battery handles rapid load variations. Simulation results using Matlab/Simulink demonstrate the effective performance of the proposed controller under different loads and input variations, showcasing improved performance compared to conventional MPC.**

***Index Terms*—Hybrid energy storage systems, model predictive control, artificial neural networks, decentralized control, DC microgrids.**

Received: July 15, 2024
Accepted: December 3, 2024
Published Online: July 1, 2025

Dongran Song, Asifa Yousaf, Javeria Noor, Yuan Cao (corresponding author), Mi Dong, and Jian Yang are with the School of Automation, Central South University, Changsha 410083, China (e-mail: humble_szy@163.com; asifayusuf76@gmail.com; javeranoor19@gmail.com; caoyuan3116@csu.edu.cn; mi.dong@csu.edu.cn; jian.yang@csu.edu.cn).

Rizk M. Rizk-Allah is with the Department of Basic Engineering Science, Faculty of Engineering, Menoufia University, Shebin El-Komm 32511, Egypt; and also with Scientific Research Group in Egypt (SRGE), Cairo 11787, Egypt (e-mail: rizk_masoud@yahoo.com).

M. H. Elkholy is with the Department of Electrical and Electronics Engineering, University of the Ryukyus, Okinawa 9030213, Japan (e-mail: melkholy094@yahoo.com).

M. Talaat is with the Electrical Power and Machines Department, Faculty of Engineering, Zagazig University, Zagazig 44519, Egypt; and also with the Faculty of Engineering and Technology, Egyptian Chinese University, Cairo 11787, Egypt (e-mail: m_mtalaat@eng.zu.edu.eg).

DOI: 10.23919/PCMP.2024.000074

I. Introduction

Microgrids are becoming increasingly popular due to their increased efficiency, and simplicity of integration with renewable energy resources (RES) and energy storage systems (ESS) [1]. DC microgrids offer a wide range of applications in residential, commercial areas and power systems due to their versatility, excellent efficiency, and high-power density supply [2]. Ensuring power supply-demand balance in DC microgrids is crucial, especially considering the fluctuations of renewable generations and sudden variations in demand [3].

To address power imbalance, ESS are widely deployed [4], [5]. In DC microgrids, fuel cells (FC) are valuable due to their high efficiency and reliable power generation. However, it is important to recognize that different ESS exhibit varying characteristics. For instance, supercapacitors (SC) possess high power density and fast dynamics but poor energy density, whereas FC possesses high energy density but slow dynamic reaction and low power density. Batteries on the other hand, have both high-energy and high-power densities [6]. To overcome the limitations of any single type of ESS in DC microgrids, researchers have introduced hybrid energy storage systems (HESS), that utilize several technologies and offer numerous benefits over a single ESS [7]. Furthermore, due to mature technology, lithium-ion batteries are more cost-effective than SC while also offer a longer lifecycle compared to other battery chemistries. Lithium-ion batteries can maintain a high state of health over time through repeated charge-discharge cycles, and thus, the FC-battery HESS is a better option than alternatives [8].

Real-time allocation of power is crucial in DC microgrids with HESS for their optimal usage [9]. Numerous research studies are presently being conducted to establish effective management for HESS including centralized, hierarchical, and decentralized control. Centralized methods, such as multi-level communication method [10], low pass filter method [11], and fuzzy-logic based method [12], need a central controller to create reference signals for each specific ESS converter controller via communication systems. However, this approach can lead to intricate system design and

thus is not optimal for scalability. The decentralized method is preferable to improve system performance because it does not rely on communication systems to regulate power [13].

Among the latest control methods, model predictive control (MPC) is considered to be one of the best advanced control techniques for DC microgrids with HESS compared to traditional controllers such as proportional-integral-derivative (PID) [14]. MPC-based controller is presented in [15] to solve instability issue with limited simulations. A decentralized composite MPC control for battery-SC is also designed in [16]. However, to obtain optimal control actions, the MPC requires the entire system state-space representation and results in very high computational difficulties.

MPC can be described into two types, finite control set MPC (FCS-MPC) and continuous control set MPC (CCS-MPC). In FCS-MPC, selecting a single switching state per sampling period leads to high power ripple and variable switching frequencies [17]. In contrast, CCS-MPC maintains a constant switching frequency by employing a modulator and utilizes a pulse width modulator (PWM) to generate control signals [18]. The control action for each power switch is composed of a duty cycle, and the switches can therefore have a fixed switching frequency and several states during a single sample period.

The integration of intelligent approaches has also gained prominence in addressing control challenges in DC microgrids [19]. Specifically, artificial neural networks (ANN) based controllers have been widely used for problem detection and power grid stability [20], disturbance compensation in DC microgrids [21], managing the DC-bus voltage of AC/DC microgrids with low computation stress [22].

To address the challenges of computational complexities inherent in conventional MPC, ANN-based MPC is designed to improve control performance and simplify the control actions in power converter applications [23], [24]. Even though these methods work well for single energy source DC-DC converter systems, they do not address system-level coordination for multiple energy sources. ANN-MPC for HESS is designed in [25] comprising battery and SC, where the ANN dynamically determines current references based on the current state of charge (SOC) of the battery and SC, as well as the mismatch between photovoltaic (PV) production and load power. However, this strategy is not implemented in a decentralized manner. Moreover, the previously mentioned studies do not provide insights into the switching frequency dynamics of MPC. From the above literature analysis, it is imperative to design a system-level control strategy for HESS in a decentralized manner that incorporates multiple energy sources to achieve system stability and optimize control performance while minimizing computational complexity.

In this study, a novel ANN-based MPC is proposed for HESS composed of FC and battery to address the above mentioned issues such as centralized power allocation [12], and computational complexities [16] in MPC. MPC is initially designed and operated in a simulation environment. Subsequently, ANN is trained offline using data obtained from MPC, enabling it to serve as a central controller. This alleviates the need for extensive mathematical computations. The trained neural network demonstrates strong approximation capabilities and yields control performance comparable to conventional MPC. Additionally, by integrating virtual impedance droop control, decentralized power allocation among HESS is achieved, ensuring voltage stability in DC microgrids. The HESS utilizes FC for steady-state power support while the battery handles rapid variations, thus extending FC lifespan and storing surplus energy. To validate the performance of the proposed controller in terms of voltage stability and smooth transient response, the system is tested under different input-output variations. In summary, the following points outline the main features of this study.

1) This study introduces an innovative ANN-MPC approach to address the issues of conventional MPC method, such as mathematical computational complexity in coordination between multiple energy sources. The proposed ANN-MPC optimizes control accuracy through squared error minimization and backpropagation during ANN training. Offline convergence ensures rapid dynamic response, enhancing the control performance under uncertain conditions. In addition, system model of HESS is not necessarily required.

2) To address the issue of excessive switching frequency when the switching frequency approaches the sampling frequency in FCS-MPC, a cost function is defined to incorporate a weighting factor to penalize deviations from the desired switching frequency, ultimately enhancing control performance of HESS. By limiting the switching frequency, stability is maintained and excessive switching losses are prevented.

3) To achieve decentralized power allocation among the FC and battery, a composite virtual resistance and capacitance droop control with ANN-MPC is introduced. Voltage reference signals are generated for the DC-DC converter by considering the droop relationship between the output-voltage and output-current that regulates the DC bus voltage concerning changes in the load current. Optimal tracking of the reference signal is achieved by the proposed ANN-MPC.

The rest of the paper is organized as follows. The hybrid system model under study is stated in Section II, while in Section III, the methodology is provided through an overview of MPC and ANN, the proposed ANN-MPC, and decentralized power sharing for HESS using virtual impedance droop control. Section IV in-

cludes case studies on various input-output variations, discussions on the results. Finally, Section V draws conclusions.

II. DC Microgrid with Hybrid Energy Storage System Under Consideration

The schematic design of the DC microgrid incorporating the HESS is shown in Fig. 1. A bidirectional DC-DC converter and a boost converter connect a battery and a FC to the DC bus, respectively. PV is a renewable energy source, coupled to the DC bus via a boost converter operating in maximum power point tracking mode. The DC bus is then connected to the loads.

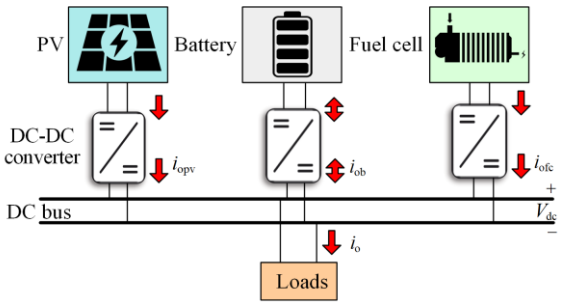

Fig. 1. Schematic design of DC microgrid with hybrid energy storage system.

The HESS maintains the power balance on the DC bus and compensates any power fluctuations between PV and loads. The DC bus currents are shown as:

$$i_{ob} + i_{ofc} = i_o \tag{1}$$

$$i_o = \frac{P_{cpl}}{V_{dc}} + \frac{V_{dc}}{R} \tag{2}$$

where i_{ob} and i_{ofc} are the resulting output currents of the battery and FC converters, respectively; i_o is the total load current; V_{dc} is the voltage on the DC bus; P_{cpl} is the power of the constant power load (CPL) which can be positive or negative; and R represents the resistive load.

The reduced schematic design of HESS under study is shown in Fig. 2. Herein, the HESS model can be stated as:

$$L_x \frac{\mathrm{d}i_{Lx}}{\mathrm{d}t} = V_x - (1 - D_x)V_{ox} \tag{3}$$

$$C_x \frac{\mathrm{d}V_{ox}}{\mathrm{d}t} = (1 - D_x)i_{Lx} - i_{ox} \tag{4}$$

where V_x, V_{ox}, i_{ox}, i_{Lx}, L_x, and C_x (x is b or fc) are the respective input voltage, output voltage, output current, inductor current, inductor value, and capacitor value of the HESS DC-DC converters; and D_x (x is b or fc) is the control signal for the switches of the battery and FC converters.

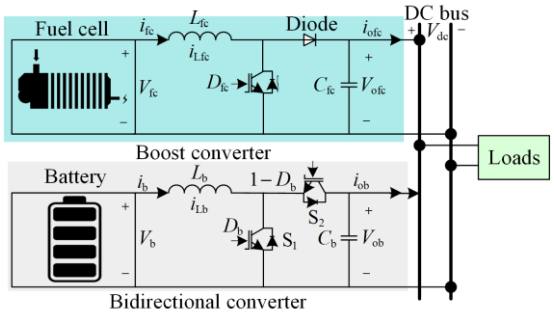

Fig. 2. Simplified DC microgrid including hybrid energy storage system.

III. Proposed ANN Based Model Predictive Control

In this study, a novel approach leveraging ANN-based MPC for HESS comprising FC and battery is proposed. The key challenges such as centralized power allocation and computational complexities, in traditional MPC methods for HESS are addressed. Initially, MPC is designed and tested in a simulation environment. Subsequently, an ANN is trained offline using data generated from MPC simulations. This trained ANN serves as a central controller within the PWM framework. To accomplish decentralized power allocation among the HESS, ANN-MPC is incorporated with virtual impedance droop control. The framework of the proposed control method is illustrated in Fig. 3, which includes two phases of operation: offline phase and online phase. In both online and offline phases, the input to the system is derived from the DC-DC converters, and the output is generated in the form of control signals for the converters.

1) The offline phase is initiated with the implementation of conventional MPC designed for the HESS, where the discrete time model of the system, prediction horizon, and cost functions are defined. This involves selecting appropriate control and prediction horizons, formulating a cost function to be minimized, and solving an optimization problem to obtain control inputs. The offline phase concludes with the generation of input-output pairs forming the dataset and ANN is then trained using this dataset.

2) In the online phase, the ANN assumes the role of the primary controller for the HESS. During training in the offline phase, the ANN learns from the dataset provided by the MPC which represents critical system states and corresponding control actions. The training process refines the internal parameters of the ANN, allowing it to capture complex relationships between input-output pairs. The trained ANN leverages this acquired knowledge to make real-time decisions and control the DC-DC converters. Moreover, the reference signals are generated based on virtual resistance and capacitance droop control designed for the FC and battery to achieve power-sharing among them in a decentralized way.

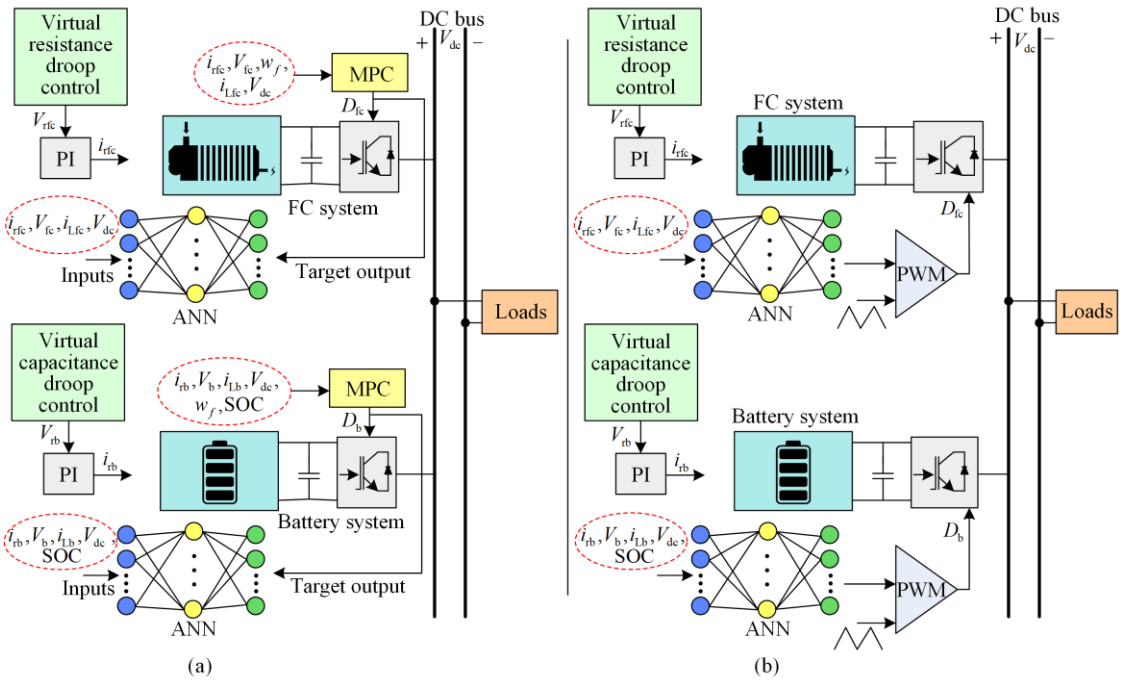

Fig. 3. Proposed ANN based model predictive control. (a) Offline phase. (b) Online phase.

A. Basis of Model Predictive Control for DC Microgrid

1) Model Predictive Control

MPC stands as a widely recognized and effective model-based control approach in the context of power electronics. It is an advanced control method characterized by its ability to handle constraints effectively [26].

The system to be controlled consists of power converters with n switching modes. Prediction and optimization are the two sections that form the MPC [27]. Considering $x(k)$ represents the system state at the start of each usual sample period $t = kT$ and $y(k)$ indicates the desired output to reach a specific reference signal $x^{\mathrm{r}}(k)$, MPC aims to calculate the control signal $D(k)$ through computational optimization based on the system output $y(k)$ and its reference signal $x^{\mathrm{r}}(k)$. This process involves finding the best control signal along a prediction horizon p spanning time frames to achieve best performance according to a predefined cost function. Upon applying the control signal $D(k)$, the system adapts to a new state $x(k+1)$, and then the procedure repeats [28].

MPC is characterized by two primary parameters, including the control horizon $m_{\mathrm{c}} \in [1, m_{\mathrm{p}}]$, representing the number of control actions to optimize in each step and the prediction horizon denoted as m_{p}, which determines how far into the future the controller looks when optimizing the control action. The cost function g consists of the error signal, which quantifies the difference between the measured output voltage and the reference value, and is given as:

$$g = \sum_{j=1}^{m_{\mathrm{y}}} \sum_{i=1}^{m_{\mathrm{p}}} \alpha_j \left[(x^{\mathrm{r}}(k))^2 - y(k))^2 \right] \tag{5}$$

where α_j represents the weighting parameter which is used in fine-tuning the MPC system; and m_{y} is the number of control outputs.

2) Model Predictive Control Implementation for Hybrid Energy Storage System

As shown in Fig. 2, the HESS is composed of a boost converter for FC and a bidirectional converter for the battery system. Initially, FCS-MPC is designed for the HESS, so the discrete-time model of the DC-DC converters is required. For the FC system, the boost converter is used to step up the voltage.

The output voltage of the boost converter is regulated by altering the duty cycle of switch S. In MPC, the pulse for the switch is generated directly by the MPC. The switching modes of the switch S are defined by D_{fc} as:

$$D_{\mathrm{fc}} = \begin{cases} 1, & \text{if } s = 1 \\ 0, & \text{if } s = 0 \end{cases} \tag{6}$$

where $S = 1$ indicates the ON position of switch; and $S = 0$ indicates OFF position.

The discrete-time system model of the boost converter which predicts the future response of voltage and current is expressed as:

$$i_{\mathrm{Lfc}}(k+1)=(\frac{T}{L_{\mathrm{fc}}}-1)i_{\mathrm{Lfc}}(k)+(D_{\mathrm{fc}}(k)-1)\frac{T}{L_{\mathrm{fc}}}V_{\mathrm{dc}}(k) \quad (7)$$

$$V_{\mathrm{dc}}(k+1)=(1-\frac{T}{C_{\mathrm{fc}}})V_{\mathrm{dc}}(k)+\frac{T}{C_{\mathrm{fc}}}i_{\mathrm{Lfc}}(k)-\frac{T}{C_{\mathrm{fc}}}i_{\mathrm{Lfc}}(k)D_{\mathrm{fc}}(k) \quad (8)$$

where $(k+1)$ presents the next state; and T is the sampling time.

And g, chosen for this case, is illustrated as:

$$g=\left[i_{\mathrm{rfc}}(k+1)^2-i_{\mathrm{Lfc}}(k+1)\right]^2+\lambda\times\left[D_{\mathrm{fc}}(k)^2-D_{\mathrm{fc}}(k-1)\right]^2 \quad (9)$$

where i_{rfc} is the reference current for converter; and λ is the weighting factor.

The control objective contains two terms. The first term focuses on minimizing the error between the reference and the actual currents of the converter. Furthermore, as the MPC does not use comparators to generate the control output, it has a variable switching frequency. If the switching frequency is close to the sampling frequency, control error will rise [29]. To decrease the switching frequency, the second term in the cost function for switching states is adopted and λ is utilized to limit its effects on the total cost function. In this study, λ is determined as 0.15 by using the cost function classification method proposed in [30]. The compromise between the switching frequency and the inductor current error is set by the $\lambda>0$. It is worth mentioning that the switching frequency changes according to the operating point of the converter. The switching frequency is less than half of the sampling frequency, despite the operating point and the upper bound on the switching frequency is provided by the sampling interval T_{s}, i.e., $f_{\mathrm{sw}}<1/(2T_{\mathrm{s}})$ [31].

Similarly, the power delivered or absorbed by the battery is regulated by controlling the bidirectional converter. When the battery is discharging to supply power, it operates in boost mode, and when it is charging, it operates in buck mode. For the two states, the discrete-time model of the system for a sampling time T is given as follows.

when $D_{\mathrm{b}}=1$ ($S_1=1, S_2=0$):

$$i_{\mathrm{Lb}}(k+1)=i_{\mathrm{Lb}}(k)+T\frac{V_{\mathrm{b}}}{L_{\mathrm{b}}} \quad (10)$$

$$V_{\mathrm{dc}}(k+1)=V_{\mathrm{dc}}(k)+T\frac{-i_{\mathrm{b}}(k)}{C_{\mathrm{b}}} \quad (11)$$

when $D_{\mathrm{b}}=0$ ($S_1=0,\ S_2=1$):

$$i_{\mathrm{Lb}}(k+1)=i_{\mathrm{Lb}}(k)+T\frac{V_{\mathrm{b}}-V_{\mathrm{dc}}}{L_{\mathrm{b}}} \quad (12)$$

$$V_{\mathrm{dc}}(k+1)=V_{\mathrm{dc}}(k)+T\frac{i_{\mathrm{Lb}}(k)-i_{\mathrm{o}}(k)}{C_{\mathrm{b}}} \quad (13)$$

To maintain the DC bus voltage, the bidirectional converter switches to boost mode during the battery discharging process, supplying power to the DC bus. Conversely, it switches to buck mode during the charging process, drawing power from the DC bus. Thus, g can be formulated as:

$$g=\left[i_{\mathrm{rb}}(k+1)^2-i_{\mathrm{Lb}}(k+1)\right]^2+\lambda\times\left[D_{\mathrm{b}}(k)^2-D_{\mathrm{b}}(k-1)\right]^2 \quad (14)$$

where i_{rb} is the reference current for the converter.

A proportional-integral (PI) regulator is used to provide the reference for inductor current based on output voltage error. The output voltage error e can be illustrated as:

$$e=V_{\mathrm{rx}}-V_{\mathrm{ox}} \quad (15)$$

where V_{rx} (x is b or fc) denotes the reference voltage.

The PI regulator then calculates the reference current for the intended reference voltage as follows:

$$i_{\mathrm{rx}}=k_{\mathrm{p}}e+k_{\mathrm{i}}\int e\mathrm{d}t \quad (16)$$

where k_{p} and k_{i} denotes the proportional and integral parameter, respectively.

The MPC execution for the HESS can be outlined as follows.

1) At the initiation of the switching moment, V_x, $V_{\mathrm{ox}}, i_{\mathrm{ox}}, i_{\mathrm{Lx}}$, SOC and reference signals $V_{\mathrm{rx}}, i_{\mathrm{rfc}}, i_{\mathrm{rb}}$ are measured.

2) Predictions for the measured output at the next instant, $k+1$, are made for all feasible switching states.

3) Subsequently, the computation of g for all potential states and then implementation on the converter during the subsequent time step $(k+1)$ takes place. The optimization problem underlying MPC at time-step k involves minimizing g, subject to the dynamics of the converter model, yielding the optimal switching sequence for the converter $D_x(k)$. The optimization problem can be expressed as follows:

$$D_x(k)=\mathrm{argmin}\ (g) \quad (17)$$

The control method chooses the ON state for the switch if the computed cost function for the ON position of the switch is smaller than that for the OFF position.

B. ANN Based Model Predictive Control Strategy

To determine the appropriate values for the controlled variables, MPC carries out optimization and future prediction [32], which requires significant computing load and can take a long time. ANN is employed in this

work to address the shortcomings of MPC. Based on the MPC generated dataset, the ANN is taught to act as the predictive-based controller. The strategy employing MPC aims to predict future values of the plant output and utilizes an optimization method to determine the control inputs.

ANN is typically considered as a subsection of artificial intelligence that tries to replicate the thinking of the human brain. ANN excels at nonlinear prediction and has applications in the wide range of fields, including failure identification, regression problems, network identification, and modeling of real-world systems. Their adaptability and capacity for complex pattern recognition make them an effective tool in the field of machine learning [33].

1) Architecture of ANN

A mathematical connection among input parameters and outputs is a simple description of ANN, that uses learning algorithms to generate predictions based on previous information [34]. It is composed of several layers executed in parallel. The proposed ANN is a multi-layer feed-forward neural network with Levenberg-Marquardt backpropagation process, known for its fast convergence, and its output error is used to update the weight matrices and biases of ANN. Table I shows the proposed neural network specifications. In a traditional MPC setup, an observer is required to obtain feedback from the plant output, and the feedback is crucial for the controller to make informed decisions. To simplify the structure in the ANN-MPC approach, this work replaces the observer, plant modeling, and optimizer with a feed-forward neural network where information flows in a unidirectional manner from the input nodes of the network via a hidden layer and culminates in the output nodes.

TABLE I
PROPOSED NEURAL NETWORK SPECIFICATIONS

Parameters	Training configuration
Network	Feed-forward backpropagation
Training function	Trainlm
Performance function	Mean square error
Number of layers	3

As shown in Fig. 4, the network takes M input parameters (i.e., $I_m, m=1,\cdots,M$) and generates N output (i.e., $O_n, n=1,\cdots,N$). The total amount of neurons in both layers should be equal to the number of targets to be processed. The single output neuron is expressed as:

$$y = a(b + \sum_{i=1}^{M} x_i w_i) \tag{18}$$

where a represents the activation function; the weighting parameters w_i are multiplied by every input parameter x_i before being forwarded towards the hidden layer; the biases b are added to the total of the weighted data, and each neuron is then employed by a in the hidden layer.

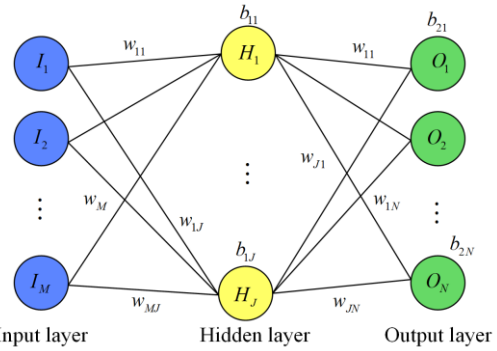

Fig. 4. Two-layer neural network architecture.

The results of this process are then multiplied by w_{mj} before fed to the output layer. a can be shifted using those biases, which enhances the capacity of the model to adapt to the provided dataset [35]. The nth output can be expressed mathematically as:

$$O_n = a\left(\sum_{j=1}^{J} w_{jn} H_j + b_{2n}\right), \forall n = \{1,\cdots,N\} \tag{19}$$

$$H_j = a\left(\sum_{m=1}^{M} w_{mj} I_m + b_{1j}\right), \forall j = \{1,\cdots,J\} \tag{20}$$

where the w_{jn} denotes the weighting parameters; the H_j represents the hidden layer outputs; and b_{2n} denotes the biases of the output layer.

To understand complex structures and evaluate how well the network design has learned the training data, a (such as sigmoid, hyperbolic tangent, softmax, and linear) is a crucial component of the ANN design [36].

2) Training of ANN

The training process of ANN is shown in Fig. 5. The most crucial step of training is the appropriate data selection. In this case, the datasets have been measured, then scaled data have been incorporated into the simulation. The collected information is used to generate input and output datasets, and then to determine the optimal values of weights w_{mj} and biases b_{1j}. To rigorously evaluate its accuracy, a standard procedure of data split process is employed. This process involves partitioning the dataset into three distinct subsets, 70% for training, 15% for testing, and another 15% for validation, at 1000 epochs.

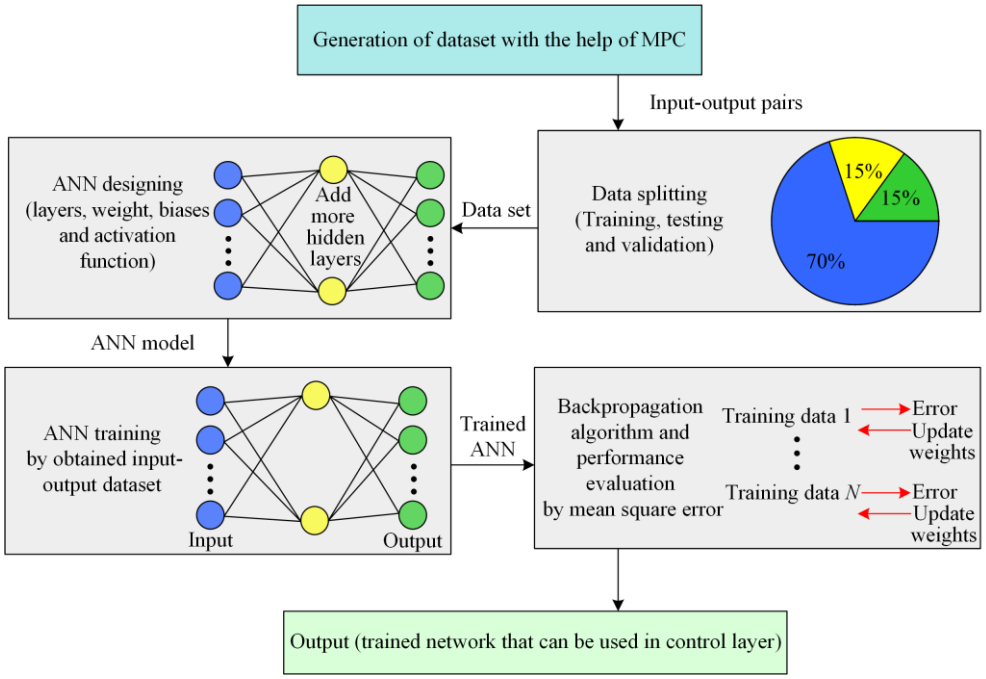

Fig. 5. ANN training steps.

The process is started with a backpropagation method containing input and output in their layers and 25 hidden neurons in the hidden layer. The training of multi-layer neural network is achieved using the Levenberg-Marquardt algorithm which is renowned for its efficiency and rapid convergence to optimal network weights. It combines the benefits of gradient descent and the Levenberg-Marquardt algorithm, ensuring rapid convergence to optimal network weights. It is important to point out that the training data measured from the system is saved into simulation as an 1000001x (number of inputs) matrix presenting data 1000001-1-time steps of input components and targeted 1000001x (number of outputs) matrix as output, presenting output data 1000001-1-time steps of one component. For the trained ANN, high accuracy can be achieved by ensuring that the value of mean squared error (MSE), i.e., e_{MSE}, is as close to 0 as possible and that the correlation coefficient (R) reflects convergence to 1. The e_{MSE} is given as:

$$e_{\mathrm{MSE}} = \frac{1}{P}\sum_{i=1}^{P}(y^*(t) - y(t))^2 \tag{21}$$

where P denotes the batch size; $y^*(t)$ denotes the solution given by MPC; and $y(t)$ denotes the solution inferred by ANN. Backpropagation is used to update the weights and bias of the ANN to reduce the loss. After ANN has been well-trained, it can mimic the continuous control behavior of MPC by generating nearly the same control as MPC. The data is obtained via MPC during the offline phase considering variable load conditions, and ANN is thoroughly trained and prepared for use during the online phase. Without requiring any computational work, the trained ANN works as a central controller for the system serving as the prediction model and generating the control signal for power converters. In simple terms, the process begins with gathering initial data for training the ANN, which is then employed to initiate operations, eliminating the requirement for additional controllers.

The optimal validation performance is assessed through the MSE value e_{MSE}, serving as the target for validation in the training process. Validation timestamps are utilized to measure network generalization and determine when to end the training procedure, stopping once further improvement ceases. One of the best validation performances of MSE for D_{fc} and D_{b} are shown in Fig. 6 and Fig. 7, respectively.

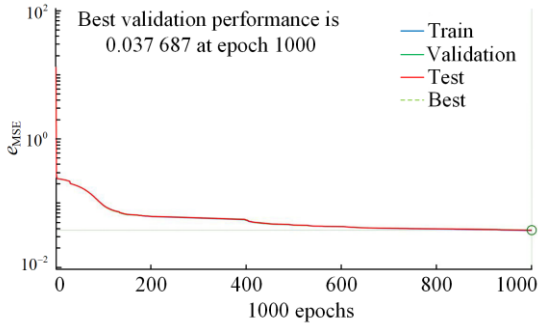

Fig. 6. e_{MSE} for D_{fc} at 1000 epochs.

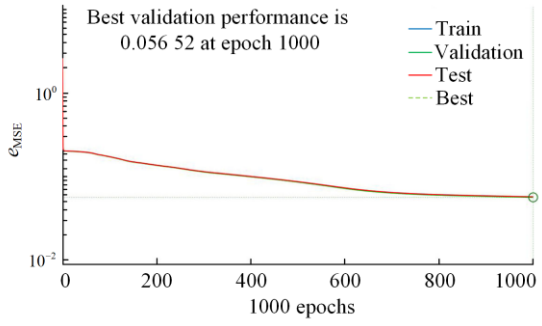

Fig. 7. e_{MSE} for D_{b} at 1000 epochs.

The inputs and outputs of ANN used to control the power converters for ESS are given in Table II with their best MSE values. The ANN-MPC method utilizes duty cycles produced by an ANN to generate PWM for power converters. These duty cycles, representing the desired on-time duration relative to the total PWM waveform period, are generated within the range of 0 to 1 by the ANN. To produce PWM signals, a carrier frequency, such as a 20 kHz triangular waveform, is employed. The ANN output is then compared with this carrier waveform to generate the PWM signals for the power converter switches.

TABLE II
ANN PARAMETERS FOR CONTROL SYSTEM OF DC-DC CONVERTERS

ANN	Control system	Input	Output	e_{MSE}
ANN for FC system	Boost converter	$V_{dc}, i_{Lfc}, i_{rfc}, V_{fc}$	D_{fc}	0.037 687
ANN for battery system	Bidirectional converter	$V_{dc}, i_{Lb}, i_{rb}, V_b$, SOC	D_b	0.056 52

C. Decentralized Power Sharing Among Hybrid Energy Storage System

The integration of the proposed ANN-MPC and virtual impedance droop control for managing the power sharing between the FC and battery is shown in Fig. 8. In the context of the virtual impedance droop control, the output voltage reference for the DC-DC converters is dynamically adjusted based on the reference DC bus voltage V^{r}, virtual resistance R_v, virtual capacitance C_v and the output current i_{ox} [37]. A virtual resistance droop control is incorporated into the integrated control system for the FC and virtual capacitance droop control for the battery. The output signal is used as a voltage reference for the DC-DC converters in both online and offline phases. This integrated approach facilitates power allocation within the HESS without any communication between them, and the DC-DC converters can track their reference signals effectively. This feature becomes particularly advantageous during dynamic load changes, preventing undue stress on the FC and mitigating the wear and tear associated with rapid power demand fluctuations.

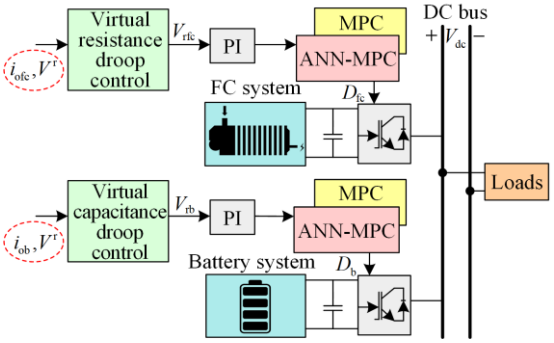

Fig. 8. Virtual impedance droop control for hybrid energy storage system.

The *V-I* characteristics of the FC converter with virtual resistance control and the battery converter with virtual capacitance characteristics are stated as:

$$V_{rfc} = V^{r} - R_v i_{ofc} \tag{22}$$

$$V_{rb} = V^{r} - \frac{1}{C_{vs}} i_{ob} \tag{23}$$

where V^{r} represents the reference DC bus voltage; R_v and C_{vs} denote virtual resistance and virtual capacitance; V_{rfc} and V_{rb} denote the reference voltage; and the output currents are denoted by i_{ofc} and i_{ob}.

Line impedance can be neglected so $V_{rfc} = V_{rb} = V_{dc}$ [38]. The output current relationship between the FC and battery can be obtained as:

$$i_{ofc} = \frac{1}{R_v C_{vS} + 1} i_o \tag{24}$$

$$i_{ob} = \frac{R_v C_{vS}}{R_v C_{vS} + 1} i_o \tag{25}$$

It is evident that the current transfer functions of the FC and battery have the traits of a high-pass and low- pass filters, respectively, and the time constant is given by:

$$T = R_v C_v \tag{26}$$

IV. SIMULATION RESULTS

To assess the effectiveness of the proposed method, simulations are carried out using Matlab/Simulink. The ANN is trained and tested first with a single ESS of FC, with dataset generated from conventional MPC, to ensure its prediction accuracy in reference signal tracking and voltage stability. The parameter values are given in Table III.

TABLE III
SYSTEM PARAMETERS VALUES

Parameter	Description	Value
V^{r}(V)	Reference voltage	100
T(us)	Sampling time	10
f_s(kHz)	Switching frequency	20
L_{fc}(μH)	Inductance	930
C_{fc}(μF)	Capacitance	1000
L_b(μH)	Inductance	575
C_b(μF)	Capacitance	1000
R_v	Virtual resistance	0.5
C_v	Virtual capacitance	1/0.5/(2π×0.5)
k_p, k_i	Proportional and integral gain	0.3, 80

A. Case Studies

1) Case 1: Voltage Stability under Variable Loads Conditions

In case 1, stability and dynamics analyses under variable load conditions are examined. The role of the ANN-MPC is to maintain voltage stability when load varies. Figure 9 illustrates the scenario when the resistive load changes from 500 W to 1000 W at 0.03 s,

and then returns to 500 W at 0.06 s. During the load transitions, a brief voltage deviation occurs, but the output voltage promptly recovers, stabilizing back to its reference value of 100 V. The control signals for both MPC and ANN-MPC are also shown for the time period around 0.05 when the load is 1000 W. The ANN-MPC achieves similar performance as MPC with smooth transient response, though MPC suffers from the computational effort resulting in slower response. Notably, the switching frequency of MPC is lower than the sampling frequency so potential control errors can be addressed.

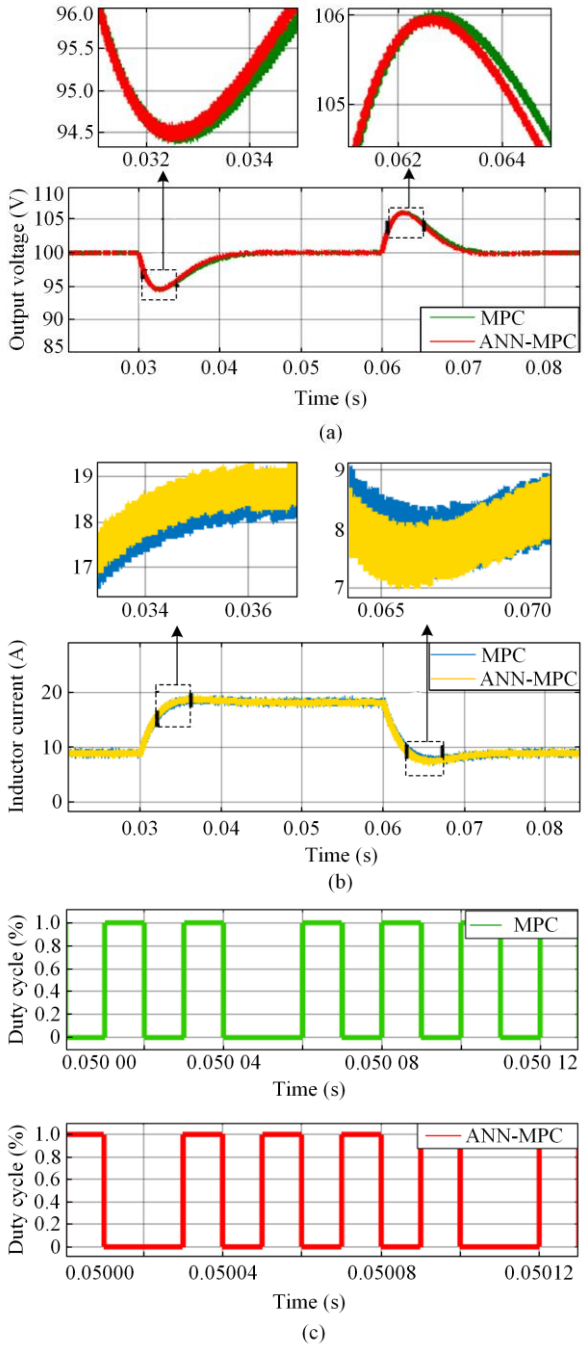

Fig. 9. Voltage stability under resistive load variations with comparison between ANN-MPC and MPC. (a) Output voltage. (b) Inductor current. (c) Control signal of MPC and ANN-MPC.

Moreover, a key challenge to system stability is the increasing use of power converters to connect loads with ESS. Many of such loads can destabilize the system due to their CPL characteristics with negative impedance. Consequently, the stability of the proposed controller is tested under variation of CPL as given in Fig. 10. At 0.03 s, the CPL changes from 500 W to 1000 W and then returns to 500 W at 0.06 s. During these load transitions, a voltage fluctuation occurs, but the output voltage quickly recovers and is stabilized to the reference voltage, showing smoother transient behavior as compared to MPC.

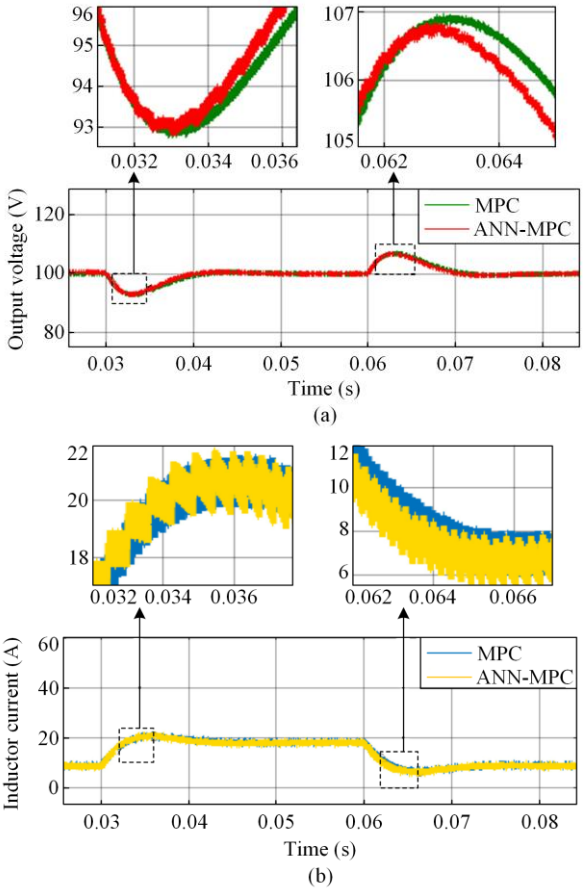

Fig. 10. Voltage stability under CPL variations with comparison between ANN-MPC and MPC. (a) Output voltage. (b) Inductor current.

2) Case 2: Voltage Stability under Input Variations

The impact of input source voltage variations on the system dynamics is assessed and the results are shown in Fig. 11. The resistive load remains constant at 500 W, while at 0.03 s, the input voltage is increased from 50 V to 70 V, and then decreased to 50 V at 0.06 s. It can be seen that the change of the source voltage causes a momentary change in the load voltage which is quickly stabilized to its reference value. Hence, system stability can be achieved in the event of input voltage variations. A comparative analysis between the ANN-MPC and MPC is performed, focusing on smooth transient response and voltage stability under varying source conditions and the precise tracking of reference signal.

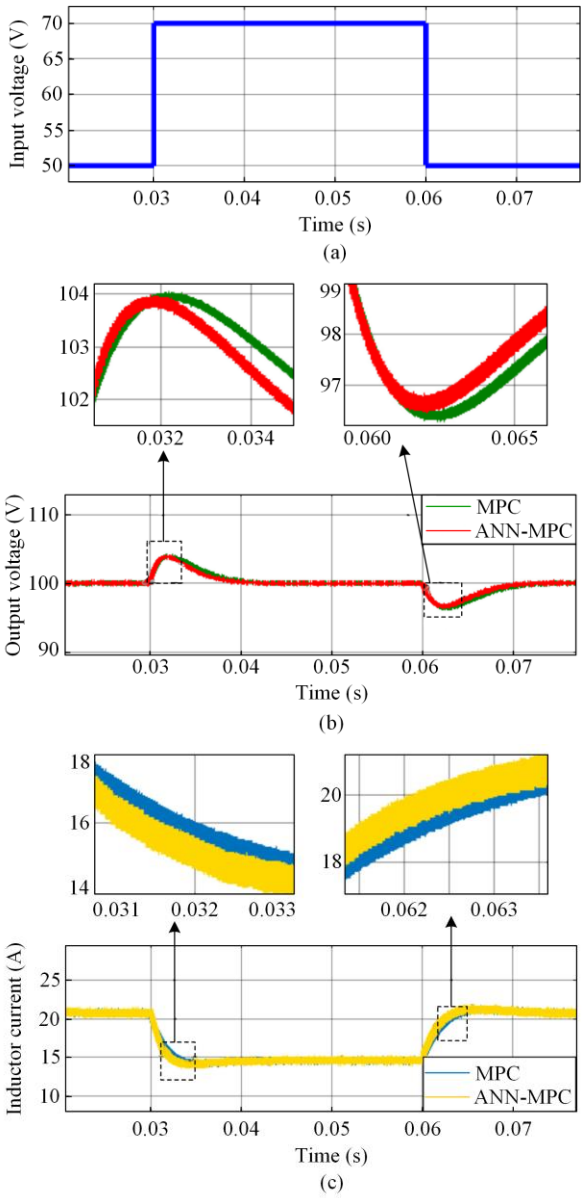

Fig. 11. Voltage stability under input source variations with a comparison between ANN-MPC and MPC. (a) Variable input source voltage. (b) Output voltage. (c) Inductor current.

The response of the controller to a varying reference signal is shown in Fig. 12 when the resistive load remains constant at 500 W. The reference voltage signal increases from 90 V to 110 V and then to 130 V at 0.03 s and 0.06 s, and finally decreases to 90 V at 0.09 s. The effective tracking capability of the proposed controller can be observed as the output voltage precisely follows the variable reference signal.

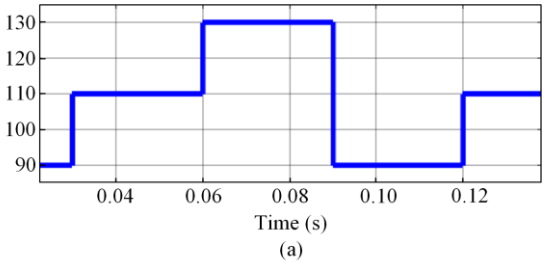

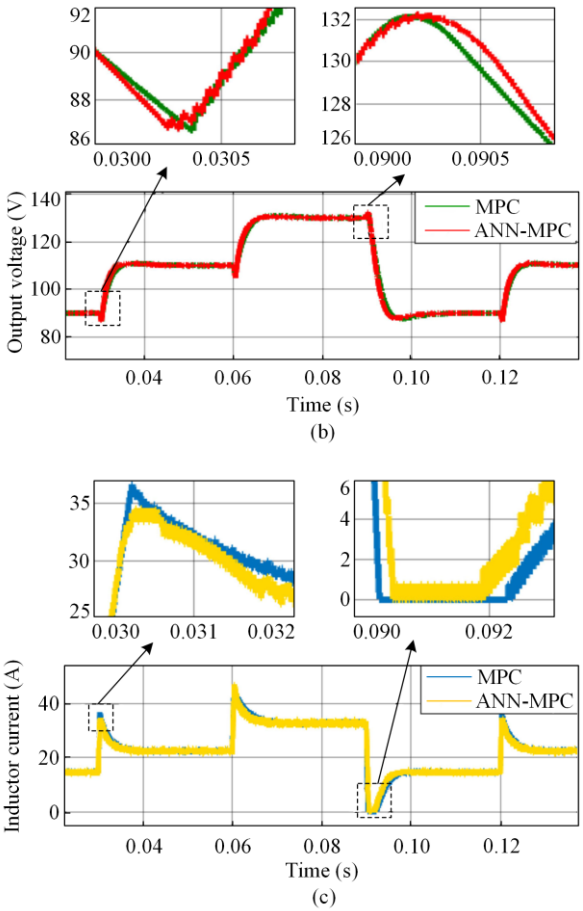

Fig. 12. Voltage stability under reference signal variations with comparison between ANN-MPC and MPC. (a) Reference voltage signal. (b) Output voltage. (c) Inductor current.

3) Case 3: Robustness Test

In evaluating the robustness of the proposed controller against parametric uncertainties, this case study considers deviations in both inductance L and capacitance C. When the L and C values differ from those used to tune the conventional MPC controller and train the ANN controller, the ANN-MPC controller exhibits strong adaptive ability to withstand the increase or decrease in L and C values beyond the nominal values.

ΔL and ΔC represent the different deviations of inductance and capacitance at −10%, 0 and +10%. Figures 13 and 14 illustrate the system response, demonstrating the gradual and smooth transitions in output voltage and inductor current as the parameters of L and C vary. Notably, the DC bus voltage remains stable, particularly during resistive load transitions from 500 W to 1000 W at 0.03 s, followed by a return to 500 W at 0.06 s. Despite these parametric changes, the system consistently maintains stable reference voltage tracking, underscoring the robustness of the proposed approach.

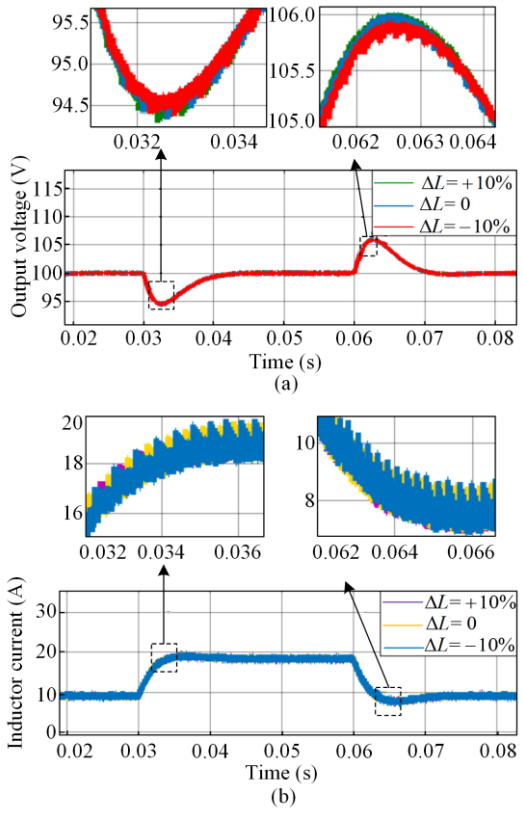

Fig. 13. Robustness test with L uncertainties. (a) Output voltage. (b) Inductor current.

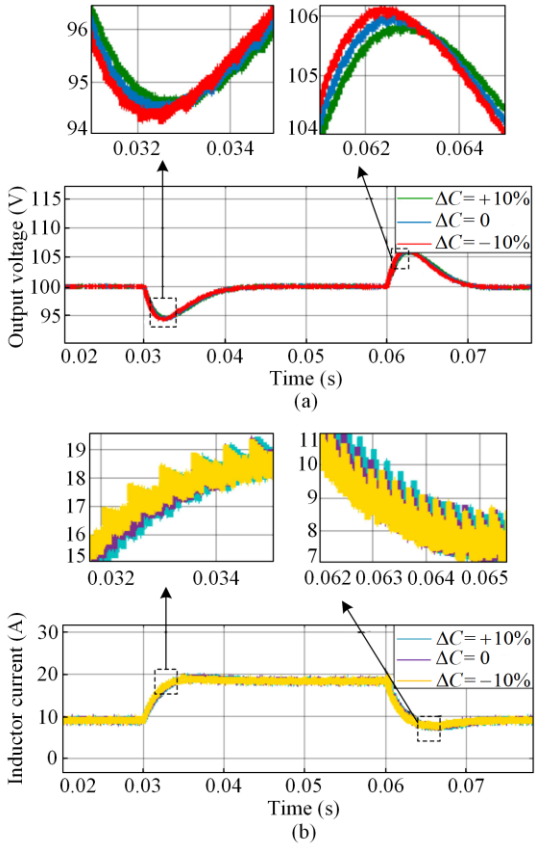

Fig. 14. Robustness test with C uncertainties. (a) Output voltage. (b) Inductor current.

4) Case 4: Decentralized Power Sharing Among HESS under Different Load Scenarios

In this case, the power-sharing within the HESS is analyzed when the resistive load undergoes a transition from 500 W to 1000 W at 1 s and then returns to 500 W at 2 s as shown in Fig. 15. In normal conditions, this load increase induces a transient current spike in the FC, which may cause demage. To mitigate this issue, a load-sharing strategy employing virtual impedance droop control between the battery and FC is implemented. It can be observed that upon sudden load change, the battery current responds promptly, while the FC current exhibits a smooth increase and decrease.

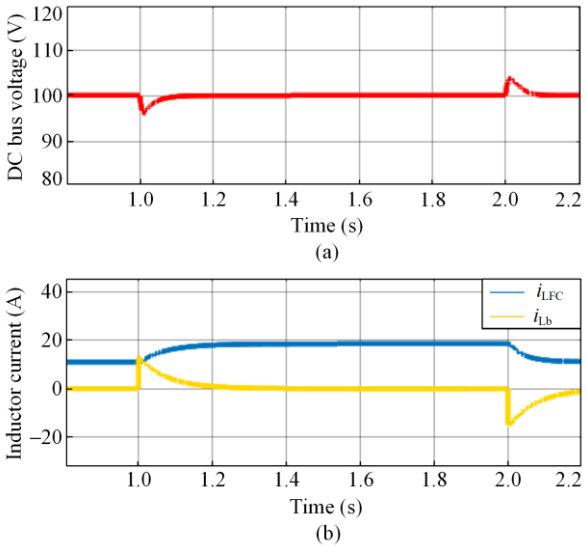

Fig. 15. Power sharing among hybrid energy storage system with resistive load. (a) Output DC bus voltage. (b) Inductor current of FC and battery.

The steady-state power supply is handled solely by the FC, with the battery contributing only during peak transients. This exemplifies the decentralized power-sharing mechanism within the HESS.

Similarly, the effectiveness of power sharing with the proposed controller is tested under variation of CPL as given in Fig. 16. At 1 s, the CPL changes from 500 W to 1000 W and then returns to 500 W at 2 s. Effective power sharing among the FC and battery is achieved with CPL. This successful adaptation to CPL variations highlights the resilience of the proposed controller in addressing transient changes, which is a crucial aspect for the reliable and efficient operation of HESS in DC microgrids.

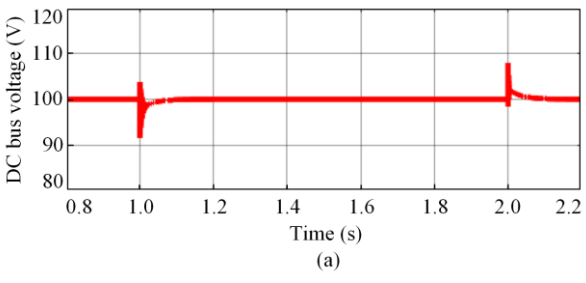

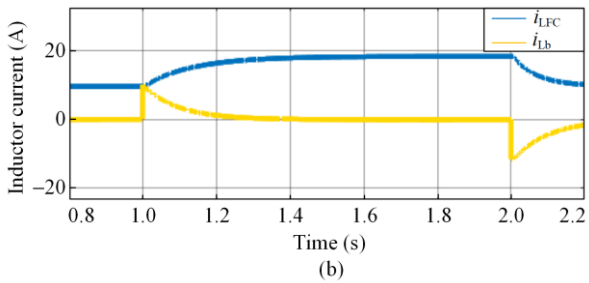

Fig. 16. Power sharing among hybrid energy storage system with CPL. (a) Output DC bus voltage. (b) Inductor current of FC and battery.

B. Numerical Results and Discussion

The numerical results are presented in Table IV which compare the MPC and ANN-MPC on DC bus voltage stability. The response time for the ANN-MPC is notably shorter, averaging 12.65 ms compared to 15.49 ms for the MPC. Additionally, the voltage overshoot is reduced with ANN-MPC, averaging ±4.78 V compared to ±4.96 V with the MPC. Moreover, the proposed controller can achieve robustness to L and C uncertainties. Furthermore, the computational complexity of the ANN-MPC is lower compared to the MPC, indicating that the ANN-MPC offers a more computationally efficient solution for the HESS.

TABLE IV
COMPARISON BETWEEN MPC AND ANN-MPC FOR DC BUS VOLTAGE

Parameter	MPC	ANN-MPC
Transient response	Average 15.49 ms	Average 12.65 ms
Voltage overshoot	Average ± 4.96 V	Average ±4.78 V
Robustness	Average	Better
Computational complexity	High	Low

The results indicate that the proposed ANN-MPC offers comparable performance to the MPC while exhibiting superior transient response and robustness against input and output variations, thereby enhancing overall system performance. Furthermore, the integration of ANN-MPC with virtual impedance droop control offers an effective solution for achieving power sharing between the FC and batteries within the DC microgrid under different load variations. The integration is achieved seamlessly, requiring no explicit communication between the FC and the battery systems. The utilization of the HESS becomes notably effective in preventing power imbalance issues in the DC microgrid.

V. CONCLUSION

This study presents a novel approach which integrates ANN-based MPC with a decentralized power sharing strategy for HESS in DC microgrids. By employing MPC as an expert to train the ANN, the proposed technique streamlines control processes and eliminates the need for complex mathematical computations associated with conventional MPC methods. By developing decentralized control scheme incorporating virtual resistance droop control for FC and virtual capacitance droop control for batteries, the HESS effectively manages power sharing, extends system lifespan, and ensures stability. Simulation results confirm the efficacy of the proposed controller, demonstrating smooth transient behavior. For future work, optimization techniques can be explored to further enhance the capabilities of the ANN-MPC, such as stochastic gradient descent with momentum, adaptive gradient algorithm, and root mean square propagation. Additionally, the optimized network architecture can be obtained by adjusting the number of layers, neurons per layer, and activation functions, and by refining the learning process for even greater computational efficiency.

ACKNOWLEDGMENT

Not applicable.

AUTHORS' CONTRIBUTIONS

Dongran Song: conceptualization, methodology, and supervision. Asifa Yousaf: methodology, validation, simulation, and writing original draft. Javeria Noor: validation and writing-reviewing. Yuan Cao: conceptualization, methodology, and writing-reviewing. Mi Dong and Jian Yang: supervision. Rizk M. Rizk-Allah: writing-reviewing and editing. M. H. Elkholy and M. Talaat: reviewing and editing. All authors read and approved the final manuscript.

FUNDING

This work is supported by the National Natural Science Foundation (NNSF) of China (No. 62103443), and Hunan Natural Science Foundation (No. 2022JJ40630).

AVAILABILITY OF DATA AND MATERIALS

Not applicable.

DECLARATIONS

Competing interests: The authors declare that they have no known competing financial interests or personal relationships that could have appeared to influence the work reported in this article.

AUTHORS' INFORMATION

Dongran Song received the B.S., M.S., and Ph.D. degrees in control science and engineering from the School of Information Science and Engineering, Central South University, Changsha, China, in 2006, 2009, and 2016, respectively. Since 2018, he has been with Central South University, Changsha, China, where he is currently a professor with the School of Automation. He

was a senior engineer with China Ming Yang Wind Power, Zhongshan, from 2009 to 2017, where he took part in the control and electrical system design of 1.5 MW–6.0 MW series wind turbines. His research interests include wind turbine control, power electronics control, and renewable energy system modeling and design.

Asifa Yousaf received the B.S. degree in electronics engineering from International Islamic University, Islamabad, Pakistan, and M.S. degree in control science and engineering from Central South University, Changsha, China in 2018 and 2024, respectively. Her research interest includes power electronics, advanced control of hybrid energy storage systems, and AI applications for DC microgrids.

Javeria Noor received the B.S. degree in electronics engineering from International Islamic University, Islamabad, Pakistan, and M.S. degree in control science and engineering from Central South University, Changsha, China in 2018 and 2024, respectively. Her research interest includes power electronics, advanced control systems for DC microgrids, and energy storage systems.

Yuan Cao received the B.S. and M.S. degrees from Central South University, Changsha, China, in 2011 and 2014, respectively, and the Ph.D. degree from the Department of Electrical and Computer Engineering, The University of Alabama, Tuscaloosa, AL, USA, in 2019, all in electrical engineering. He is currently an associate professor with the School of Automation, Central South University. Before that, he was with Baidu, USA, Hyperloop Technologies, and SANY Group. His research interests include energy storage, battery management systems, and power electronics. He received the Graduate Council Fellowship Award, in 2015 and 2017, respectively. He also received the outstanding student from the College of Engineering, the University of Alabama, in 2018 and 2019.

Mi Dong received the Ph.D. degree in control theory and control engineering from the School of Information Science and Engineering, Central South University, Changsha, China, in 2007. Since 1999, she has been with Central South University, where she is currently a professor with the School of Automation. Her research interests include control application, solar photovoltaic power generation system, and power grid power quality.

Jian Yang received the Ph.D. degree in electrical engineering from the University of Central Florida, Orlando, in 2008. He was a senior electrical engineer with Delta Tau Data Systems, Inc., Los Angeles, CA, from 2007 to 2010. Since 2011, he has been with Central South University, Changsha, China, where he is currently a professor with the School of Automation. His main research interests include control application, motion planning, and power electronics.

Rizk M. Rizk-Allah received the B.Sc., M.Sc. and Ph.D. degrees in engineering mathematics from Menoufia University, Egypt in 2004, 2010 and 2018 respectively. Since 2018, he has been an associate professor with the Department of Basic Engineering Science, Faculty of Engineering, Menoufia University, and Scientific Research Group in Egypt (SRGE), Egypt. His main research interests include engineering mathematics and artificial intelligence.

M. H. Elkholy received the B.Sc. and M.Sc. degrees from the Faculty of Engineering, Zagazig University, Egypt in 2016 and 2019 respectively. Now, he is a Ph.D. student at the Department of Electrical and Electronics Engineering, University of the Ryukyus, Japan. His research interest covers different types of energy management systems, smart grids, electric vehicle-to-grid integration, and artificial intelligence.

M. Talaat received the B.Sc., M.Sc. and Ph.D. degrees in electrical power and machines engineering from the Faculty of Engineering, Zagazig University, Egypt in 2000, 2005 and 2009 respectively. Since 2021, he has been full professor of electrical power systems at the Electrical Power and Machines Department, Faculty of Engineering, Zagazig University, Egypt. and now he is the dean of the Faculty of Engineering and Technology, Egyptian Chinese University, Cairo, Egypt. The research interest covers different types of renewable energy integration techniques, energy conversion (solar-wind-wave energies) to electrical power generation, artificial intelligence applications in power systems, IoT, and hybrid cloud-based data processing for power system monitoring in smart and microgrids.

REFERENCES

[1] T. Hai, J. Zhou, and K. Muranaka, "Energy management and operational planning of renewable energy resources-based microgrid with energy saving," *Electric Power Systems Research*, vol. 214, Jan. 2023.

[2] X. Jin, Y. Shen, and Q. Zhou, "A systematic review of robust control strategies in DC microgrids," *The Electricity Journal*, vol. 35, no. 5, Jun. 2022.

[3] Y. Li, J. Wang, and C. Yan *et al.*, "Optical and electrical losses in semitransparent organic photovoltaics," *Joule*, vol. 8, no. 2, pp. 527-541, Feb. 2024.

[4] M. Haghighat, M. Niroomand, and H. D. Tafti *et al.*, "A review of state-of-the-art flexible power point tracking algorithms in photovoltaic systems for grid support: classification and application," *Journal of Modern Power Systems and Clean Energy*, vol. 12, no. 1, pp. 1-21, Jan. 2024.

[5] Z. Yang. H. Wang, and W. Liao *et al*., "Protection challenges and solutions for AC systems with renewable energy sources: a review," *Protection and Control of Modern Power Systems*, vol. 10, no. 1, pp. 18-39, Jan. 2025.

[6] Q. Song, L. Wang, and J. Chen, "A decentralized energy management strategy for a fuel cell-battery hybrid electric vehicle based on composite control," *IEEE Transaction on Industrial Electronics*, vol. 68, no. 7, pp. 5486-5496, Jul. 2021.

[7] D. Liu, Q. Yang, and Y. Chen *et al.*, "Optimal parameters and placement of hybrid energy storage systems for frequency stability improvement," *Protection and Control of Modern Power Systems*, vol. 10, no. 2, pp. 40-53, Mar. 2025.

[8] J. Gao, D. Yang, and S. Wang *et al*., "State of health estimation of lithium-ion batteries based on Mixers-bidirectional temporal convolutional neural network," *Journal of Energy Storage*, vol. 73, Dec. 2023.

[9] Y. Qiu, Q. Li, and Y. Ai *et al*., "Two-stage distributionally robust optimization-based coordinated scheduling of integrated energy system with electricity-hydrogen hybrid energy storage," *Protection and Control of Modern Power Systems*, vol. 8, no. 2, pp. 1-14, Apr. 2023.

[10] M. Badar, I. Ahmad, and A. A. Mir *et al*., "An autonomous hybrid DC microgrid with ANN-fuzzy and adaptive terminal sliding mode multi-level control structure, " *Control Engineering Practice*, vol. 121, Apr. 2022.

[11] KA. Khan, A. Atif, and M. Khalid, "Hybrid battery-supercapacitor energy storage for enhanced voltage stability in DC microgrids using autonomous control strategy, " in *Emerging Trends in Energy Storage Systems and Industrial Applications*, Pittsburgh, USA: Academic Press, 2023, pp. 535-569.

[12] S. S. Zehra, A. Ur Rahman, and I. Ahmad, "Fuzzy-barrier sliding mode control of electric-hydrogen hybrid energy storage system in DC microgrid: modelling, management and experimental investigation," *Energy*, vol. 239, Jan. 2022.

[13] C. Wang, J. Duan, and B. Fan *et al*., "Decentralized high-performance control of DC microgrids," *IEEE Transaction on Smart Grid*, vol. 10, no. 3, pp. 3355-3363, May 2019.

[14] J. Yang, T. Yang, and L. Luo *et al*., "Tracking-dispatch of a combined wind-storage system based on model predictive control and two-layer fuzzy control strategy," *Protection and Control of Modern Power Systems*, vol. 8, no. 4, pp. 1-16, Oct. 2023.

[15] Z. Karami, Q. Shafiee, and S. Sahoo *et al*., "Hybrid model predictive control of DC-DC boost converters with constant power load," *IEEE Transactions on Energy Conversion*, vol. 36, no. 2, pp. 1347-1356, Jun. 2021.

[16] M. Zhang, Q. Xu, and C. Zhang *et al*., "Decentralized coordination and stabilization of hybrid energy storage systems in DC microgrids," *IEEE Transactions on Smart Grid*, vol. 13, no. 3, pp. 1751-1761, May 2022.

[17] S. Vazquez, D. Marino, and E. Zafra *et al*., "An artificial intelligence approach for real-time tuning of weighting factors in FCS-MPC for power converters," *IEEE Transaction on Industrial Electronics*, vol. 69, no. 12, pp. 11987-11998, Dec. 2022.

[18] Y. Arias-Esquivel, R. Cárdenas, and L. Tarisciotti *et al*., "A two-step continuous-control-set MPC for modular multilevel converters operating with variable output voltage and frequency," *IEEE Transactions on Power Electronics*, vol. 38, no. 10, pp. 12091-12103, Oct. 2023.

[19] T. A. Nakabi and P. Toivanen, "Deep reinforcement learning for energy management in a microgrid with flexible demand," *Sustainable Energy, Grids and Networks*, vol. 25, Mar. 2021.

[20] N. Ma, H. Yin, and K. Wang, "Prediction of the remaining useful life of supercapacitors at different temperatures based on improved long short-term memory," *Energies*, vol. 16, no. 14, Jan. 2023.

[21] T. Zaman, Z. Feng, and S. Mitra *et al*., "ANN driven FOSMC based adaptive droop control for enhanced DC microgrid resilience," *IEEE Transaction on Industrial Applications*, pp. 1-12, Oct. 2023.

[22] N. Chettibi, A. Massi Pavan, and A. Mellit *et al*., "Real-time prediction of grid voltage and frequency using artificial neural networks: an experimental validation," *Sustainable Energy, Grids and Networks*, vol. 27, Sep. 2021.

[23] P. Ranjan Bana, M. Amin, and M. Molinas, "ANN-based surrogate pi and MPC controllers for grid-connected VSC system: small-signal analysis and comparative evaluation," *IEEE Journal of Emerging and Selected Topics in Power Electronics*, vol. 12, no. 1, pp. 566-578, Feb. 2024.

[24] Y. Xiang, H. S. H. Chung, and R. Shen *et al*., "An ANN-based output-error-driven incremental model predictive control for buck converter against parameter variations," *IEEE Journal of Emerging and Selected Topics in Power Electronics*, vol. 12, no. 2, pp. 1230-1248, Apr. 2024.

[25] J. Faria, J. Pombo, and M. do R. Calado *et al*., "Power management control strategy based on artificial neural networks for standalone PV applications with a hybrid energy storage system," *Energies*, vol. 12, no. 5, Jan. 2019.

[26] S. Negri, F. Giani, and A. Massi Pavan *et al*., "MPC-based control for a stand-alone LVDC microgrid for rural electrification," *Sustainable Energy*, *Grids and Networks*, vol. 32, Dec. 2022.

[27] S. Zhou, M. Zhu, and J. Lin *et al.*, "Discrete space vector modulation and optimized switching sequence model predictive control for three-level voltage source inverters," *Protection and Control of Modern Power Systems*, vol. 8, no. 4, pp. 1-16, Oct. 2023.

[28] X. Liu, L. Qiu, and J. Rodriguez *et al*., "Data-driven neural predictors-based robust mpc for power converters," *IEEE Transactions on Power Electronics*, vol. 37, no. 10, pp. 11650-11661, Oct. 2022.

[29] P. Karamanakos, T. Geyer, and S. Manias, "Direct model predictive current control strategy of DC–DC boost converters," *IEEE Journal of Emerging and Selected Topics in Power Electronics*, vol. 1, no. 4, pp. 337-346, Dec. 2013.

[30] J. Rodriguez and P. Cortes, "Weighting factor design," in *Predictive Control of Power Converters and Electrical Drives*, West Sussex, UK: John Wiley & Sons Ltd., 2012, pp. 163-165.

[31] N. Guler, S. Biricik, and S. Bayhan *et al*., "Model predictive control of DC–DC SEPIC converters with autotuning weighting factor," *IEEE Transactions on Industrial Electronics*, vol. 68, no. 10, pp. 9433-9443, Oct. 2021.

[32] Y. Xiang, H. S. H. Chung, and H. Lin, "Light implementation scheme of ANN-based explicit model-predictive control for DC–DC power converters," *IEEE Transactions on Industrial Informatics*, vol. 20, no. 3, pp. 4065-4078, Mar. 2024.

[33] X. Liu, L. Qiu, and Y. Fang *et al*., "Predictor-based data-driven model-free adaptive predictive control of power converters using machine learning," *IEEE Transactions on Industrial Electronics*, vol. 70, no. 8, pp.7591-7603, Aug. 2023.

[34] N. Chettibi, A. Mellit, and G. Sulligoi *et al*., "Adaptive neural network-based control of a hybrid AC/DC microgrid," *IEEE Transactions on Smart Grid*, vol. 9, no. 3, pp. 1667-1679, May 2018.

[35] W. Meng, D. Song, and L. Huang *et al*, "Distributed energy management of electric vehicle charging stations based on hierarchical pricing mechanism and aggregate feasible regions," *Energy*, vol. 289, Mar. 2024.

[36] Y. Wang, J. Tang, and J. Si *et al.*, "Power quality enhancement in islanded microgrids via closed-loop adaptive virtual impedance control," *Protection and Control of Modern Power Systems*, vol. 8, no. 1, pp. 1-17, Jan. 2023.

[37] E. Buraimoh, A. O. Aluko, and O. E. Oni *et al*., "Decentralized virtual impedance-conventional droop control for power sharing for inverter-based distributed energy resources of a microgrid," *Energies*, vol. 15, no. 12, Jan. 2022.

[38] X. Chen, J. Zhou, and M. Shi *et al*., "A novel virtual resistor and capacitor droop control for HESS in medium-voltage DC system," *IEEE Transactions on Power Systems*, vol. 34, no. 4, pp. 2518-2527, Jul. 2019.